marine drugs

MDPI

Article

Unusual Cladiellin-type Diterpenoids from the South China Sea Soft Coral *Cladiella krempfi*: Structures and Structure-Activity Relationship with EGFR

Yang Jin [1,3], Li-Gong Yao [2,3], Yue-Wei Guo [1,2,3,*] and Xu-Wen Li [1,2,3,*]

[1] School of Chinese Materia Medica, Nanjing University of Chinese Medicine, 210023 Nanjing, China; j20-jinyang-nj@simm.ac.cn (Y.J.)
[2] Drug Discovery Shandong Laboratory, Bohai Rim Advanced Research Institute for Drug Discovery, Yantai, Shandong 264117, China; yaoligong@simm.ac.cn (L.-G.Y.)
[3] State Key Laboratory of Drug Research, Shanghai Institute of Materia Medica, Chinese Academy of Sciences, 555 Zu Chong Zhi Road, Zhangjiang Hi-Tech Park, Shanghai 201203, China
* Correspondence: ywguo@simm.ac.cn (Y.-W.G.); xwli@simm.ac.cn (X.-W.L.); Tel.: +86-21-50805813

Abstract: Two new cladiellin-type diterpenoids (**1** and **2**), and four known related compounds **3**–**6**, were isolated from the South China Sea soft coral *Cladiella krempfi*. Compound **2** is the third example of cladiellins of an unusual peroxy group at C-6 position in *C. krempfi*. The structures and absolute configurations of the new compounds were established by extensive spectroscopic analysis, X-ray diffraction, and/or chemical correlation. In bioassay, all the compounds were evaluated for the cytotoxicity and the EGFR inhibitory activity. Molecular docking experiment was conducted to study the structure-activity relationship of cladiellin-type diterpenoids on EGFR inhibitory activity.

Keywords: Soft coral; *Cladiella krempfi*; Cladiellin-type diterpenoid; X-ray diffraction; Structure-Activity relationship

Citation: Jin, Y.; Yao, L.; Guo, Y.; Li, X. Uusual Cladienllin-type Diterpenoids from the South China Sea Soft Coral Cladiella krempfi: Structures and Structure-Activity Relationship with EGFR. *Mar. Drugs* **2022**, *20*, x. https://doi.org/10.3390/xxxxx

Academic Editor: Bin Wang and Chang-Feng Chi

Received: date
Accepted: date
Published: date

1. Introduction

Soft corals of the genus *Cladiella* (order Alcyonacea, family Alcyoniidae) are widely distributed in tropical Indo-Pacific area. They are rich sources of diverse and complex diterpenoids, especially 2,11-cyclized cembranoids, which are also called cladiellin or eunicellin-type diterpenoids [1]. Literature investigation indicated that cladiellins isolated from the genus *Cladiella*, mainly *Cladiella krempfi*, were divided into various classes, including those with only one (C2-C9 or C2-C6) ether bridge, with two ether bridges (C2-C9/C3-C7 or C2-C9/C12-C17), and *et al* [2]. Some of these diterpenoids also showed broad biological activities, such as anti-inflammatory [3], antifouling [4], antiproliferative [5], and cytotoxic effects [6]. Particularly, sclerophytin A showed significant cytotoxicity against mouse lymphocytic leukemia L1210 cells at a concentration as low as 1 ng/mL (Figure 1) [7]. Moreover, Epidermal growth factor receptor (EGFR), related to the inhibition of tumor cell proliferation, angiogenesis, tumor invasion, metastasis and apoptosis, was the only target protein found so far that cladiellin-type diterpenoids can play a role. For instance, Sayed and co-workers reported that pachycladin A exhibited promising EGFR inhibitory activity with IC_{50} value of 0.5 μ M (Figure 1). Therefore, cladiellins have attracted chemists and pharmacologists all over the world for their further investigation [8,9].

In our ongoing efforts on the discovery of novel and bioactive marine natural products, plenty of secondary metabolites with various biological activities were isolated from marine invertebrates [10-14], including cladiellins [5,15]. In order to obtain

more sclerophytin A and pachycladin A like new and bioactive cladiellins, *C. krempfi* was collected off the Ximao Island, Hainan Province, China, and chemically investigated, resulting in the isolation and characterization of two new cladiellin-type diterpenoids, namly litophynols C and D (**1** and **2**) (Figure 1), and four known ones (**3**–**6**). Herein, we report the isolation, structure elucidation, biological evaluation, and the structure-activity relationship (SAR) analysis of the isolates assisted by molecular docking experiment.

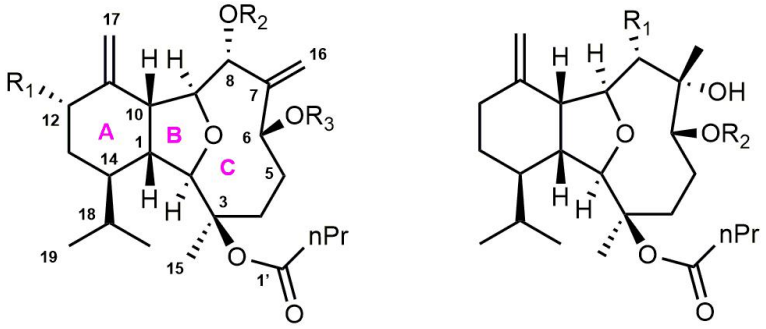

1 R_1=OH, R_2=Ac, R_3=H
2 R_1=OH, R_2=Ac, R_3=OH
3 R_1=H, R_2=H, R_3=H
4 R_1=H, R_2=nPr, R_3=H

5 R_1=OH, R_2=Me
6 R_1=H, R_2=H

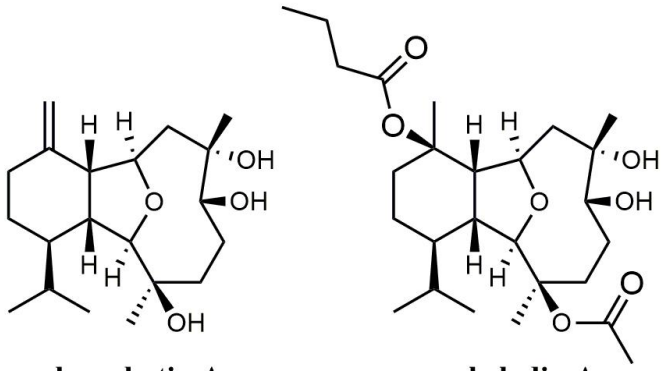

sclerophytin A **pachcladin A**

Figure 1. Structures of compounds **1**–**6** and two bioactive reference compounds sclerophytin A and pachycladin A.

2. Results and Discussion

The usual workup [16-18] of the Et_2O-soluble portion of the acetone extract of the soft coral C. krempfi yielded the pure compounds **1** (1.4 mg), **2** (5.7 mg), **3** (2.2 mg), **4** (2.0 mg), **5** (2.1 mg), and **6** (1.0 mg), respectively. The known compounds **3**–**6** were readily identified as litophynol A (**3**) [19], (1R*, 2R*, 3R*, 6R*, 8R*, 9S*, 10R*, 14R*)-3,8-dibutanoyloxycladiell-7(16), 11(17)-dien-6-ol (**4**) [15], kremfielin B (**5**) [3], and litophynin E (**6**) [20] by comparing their NMR spectroscopic data and optical rotation with those reported in the literature.

Litophynol C (**1**) was isolated as an optically active colorless oil. Its molecular formula was established as $C_{26}H_{40}O_7$ by HR-ESIMS (m/z 487.2671 $[M + Na]^+$, calcd. 487.2666), indicating seven degrees of unsaturation. The ^{13}C NMR, DEPT, and HSQC spectra of **1** revealed 26 carbon signals including five sp^3 methyls, five sp^3 methylenes, nine sp^3 methines (five oxygenated ones at δ_C 91.1, 79.2, 83.7, 71.5, and 68.4), one oxygenated sp^3 quaternary carbon (δ_C 84.7), two sp^2 methylene, and four sp^2 quaternary carbons (two ester carbonyls at δ_C 172.7 and 170.8). The diagnostic ^1H and ^{13}C NMR

resonances, as well as coupling constants of the connected protons (Table 1), indicated the presence of two disubstituted terminal double bonds [δ_H 5.37, 5.64 / δ_C 120.2（CH_2), δ_C 149.4 (qC); δ_H 4.89, 5.15 / δ_C 116.4 (CH_2), δ_C 146.1 (qC)]. Two double bonds and two ester carbonyls occupied four of the seven degrees of unsaturation, indicating a tricyclic ring system belonged to the structure.

Table 1. ^{1}H NMR (δ_H) and ^{13}C NMR (δ_C) Data for **1** and **2** in $CDCl_3$

No.	**1**		**2**	
	δ_H (mult., *J*, Hz) [a]	δ_C (mult)[b]	δ_H (mult., *J*, Hz) [a]	δ_C (mult)[b]
1	data			
2				
3		84.7		84.5
4a	1.79, m	29.8	1.88, m	29.4
4b	2.23, m		2.26, m	
5a	1.74, m	35.9	1.50, m	30.4
5b	2.20, m		2.16, m	
6	4.71, d (8.1)	68.4	4.93, dd (3.6, 11.3)	81.6
7		149.4		145.0
8	5.28, s	79.2	5.25, s	78.6
9	4.68, d (10.5)	83.7	4.65, d (10.7)	83.8
10	2.94, dd	46.6	2.96, dd (7.7, 11.1)	46.4
11		146.1		145.8
12	4.46, s	71.5	4.47, s	71.5
13a	1.27, m	30.9	1.29, m	31.1
13b	1.94, m		1.92, m	
14	1.87, m	35.6	1.89, m	35.5
15	1.60, s	22.7	1.61, s	22.7
16a	5.37, s	120.2	5.51, s	121.6
16b	5.64, s		5.66, s	
17a	4.89, brs	116.4	4.91, brs	116.7
17b	5.15, brs		5.15, brs	
18	1.92, m	27.2	1.89, m	27.2
19	0.98, d (7.0)	21.8	0.99, d (6.9)	21.8
20	0.76, d (6.8)	15.5	0.76, d (6.8)	15.4
1′		172.7		172.7
2′	2.13, m	37.5	2.14, m	37.5
3′	1.59, m	18.6	1.58, m	18.6
4′	0.93, t	13.8	0.92, t	13.8
1″		170.8		171.3
2″	2.11, s	21.6	2.06, s	21.6

[a] Recorded at 600 MHz. [b]Recorded at 125 MHz. Assignments were deduced by analysis of 1D and 2D NMR spectra

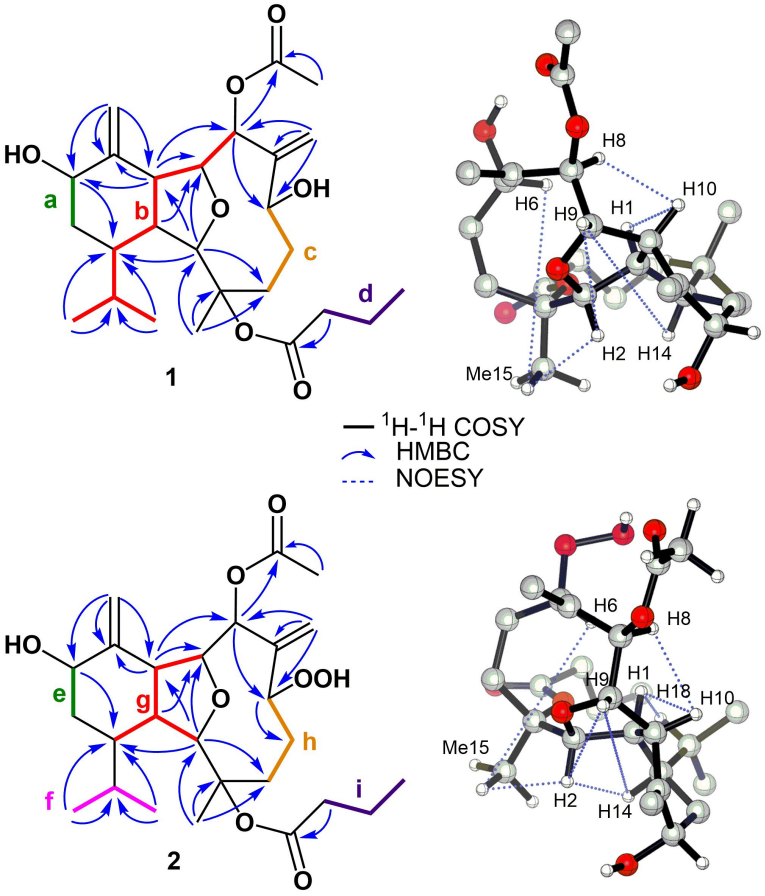

Figure 2. ^{1}H-^{1}H COSY, key HMBC, and NOESY correlations of compounds **1** and **2**.

The planar configuration of **1** was determined by ^{1}H-^{1}H COSY and HMBC experiments (Figure 2). Four structural fragments **a** – **d** were rapidly identified by carefully analyzing the ^{1}H-^{1}H COSY spectrum of **1**, with the clear correlations of H-12 (δ_H 4.46)/H_2-13 (δ_H 1.27, 1.94) (**a**); H-8 (δ_H 5.28)/H-9 (δ_H 4.68)/H-10 (δ_H 2.94)/H-1 (δ_H 2.23)/H-14 (δ_H 1.87)/H-18 (δ_H 1.89)/H_3-19 (δ_H 0.99)/H_3-20 (δ_H 0.76) (**b**); H_2-4 (δ_H 1.79, 2.23)/H_2-5 (δ_H 1.74, 2.20)/H-6 (δ_H 4.71) (**c**); H_2-2′ (δ_H 2.14)/H_2-3′ (δ_H 1.58)/H_3-4′ (δ_H 0.92) (**d**), respectively. The connection between fragments **a** – **d** was further figured out by the detailed interpretation of the well resolved HMBC spectrum (Figure 2). The HMBC correlations from H-10 to C-11/C-12, from H_2-17 to C-10/C-11/C-12 and from H-12 to C-14 revealed the presence of a cyclohexane ring (ring A) with a terminal double bond at C-11 and an isopropyl group at C-14. The cross peaks from H_3-15 to C-2/C-3/C-4 and from H-2 to C-4/C-9/C-10/C-14, revealed that the ring A and fragment **c** were connected via the C-2 and C-3. Besides, the cross peaks from H_2-16 to C-6/C-7/C-8, suggested a cyclodecane ring fused with ring A at C-1 and C-10. Furthermore, the strong correlation from H-2 to C-9 and the remaining degree of unsaturation were all indicated an ether bridge between C-2 and C-9, which divided the cyclodecane ring into a tetrahydrofuran ring B and an oxocane ring C. Finally, the acetyl group at C-8 was deduced by the HMBC correlation from H-8 to C-1″ and from H_3-2″ to C-1″, which also suggested that the connection of the rest butyryl group should be at C-3. Thus, the planar structure of **1** was determined as shown in Figure 1.

The relative configuration of **1** was established by analysis of its NOESY spectrum (Figure 2). As the orientation of H-1 of all the reported cladiellin-type diterpenoids was determined as *β* [20], that of compound **1** was also arbitrarily assigned as *β*-configuration. The NOE correlation of H-1/H-10 and H-10/H-8 suggested that H-8, and H-10 were all *β*-configuration. In addition, the cross peaks of H-6/H_3-15, H_3-15/H-2,

H-2/H-9, and H-9/H-14 indicated the α-configuration of the H-6, Me-15, H-2, H-9, and H-14. Above all, the relative configuration of **1** was ambiguously deduced as 1*R**, 2*R**, 3*R**, 6*R**, 8*R**, 9*S**, 10*R** and 14*R**. Due to the confused NOE correlations between adjacent H signals, the orientation of the rest H-12 was still hard to define.

In order to confirm the absolute configuration of **1**, we have tried many efforts and fortunately obtained its signal crystal from the recrystallization of **1** in methanol, which allowed a successful performance of X-ray crystallography study using Cu Kα radiation (λ = 1.54178 Å). Analysis of the X-ray data unambiguously confirmed the planar structure of **1**, and determined its absolute configuration as 1*R*, 2*R*, 3*R*, 6*R*, 8*R*, 9*S*, 10*R*, 12*S*, 14*R* [Flack parameter was 0.04(13)] (Figure 3). Thus, the structure of **1** was determined, namely litophynol C (Figure 1).

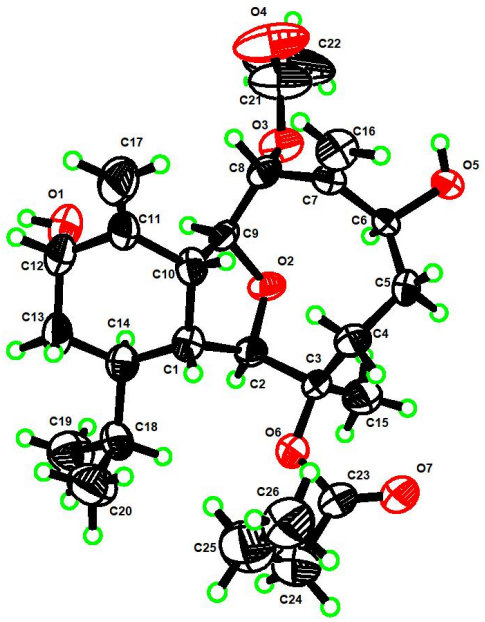

Figure 3. Perspective ORTEP drawing of X-ray structures of **1** (displacement ellipsoids are drawn at the 50% probability level).

Litophynol D (**2**) was isolated as an optically active colorless oil. Its molecular formula was established as $C_{26}H_{40}O_8$ by HR-ESIMS (*m*/*z* 503.2618 [M + Na]$^+$, calcd. 503.2615), indicating the presence of seven degrees of unsaturation. The ^{13}C NMR, DEPT, and HSQC spectra of **2** revealed 26 carbon signals, including five sp^3 methyls, five sp^3 methylenes, nine sp^3 methines, one oxygenated sp^3 quaternary carbon, two sp^2 methylene, and four sp^2 quaternary carbons. In fact, as shown in Table 1, the NMR data of **2** were extremely closed to those of **1**, indicating that they are structure analogs. After the careful comparison of 1D and 2D NMR spectra, the mainly differences between **1** and **2** were found to the downfield shift of C-6 from $\delta_{C/H}$ 68.4/4.71 in **1** to 81.6/4.93 in **2**, and its surrounding carbons, e.g. C-5 from $\delta_{C/H}$ 35.9/1.74, 2.20 in **1** to 30.4/1.50, 2.16 in **2**; C-7 from δ_C 149.4 in **1** to 145.0 in **2**, which strongly implying the hydroxyl at C-6 in **1** was replaced by the hydroperoxide group in **2**. The 16 mass units more of the molecular weight in **2** further supported our determination. The detailed 2D NMR analyses as shown in Figure 2 confirmed the planar structure and relative configuration of **2.**

To further confirm our assignment, triphenylphosphine was used to convert the hydroperoxide group of **2** into the corresponding alcohol in $CDCl_3$ (Scheme 1). The reduction of **2** resulted in a compound identical [^{1}H NMR (Figure 4) and MS data (Figure S30)] to **1**. Thus, the absolute configuration of **2** was unambiguously determined to be the same as that of **1** (Figure 1).

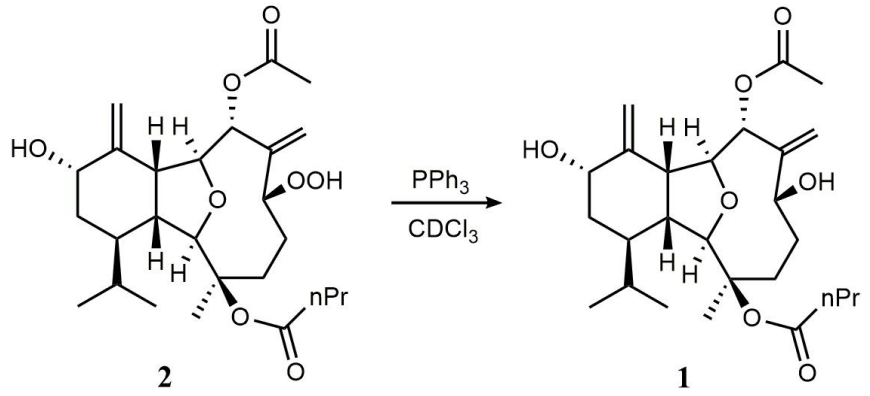

Scheme 1. Reduction of **2** to **1**.

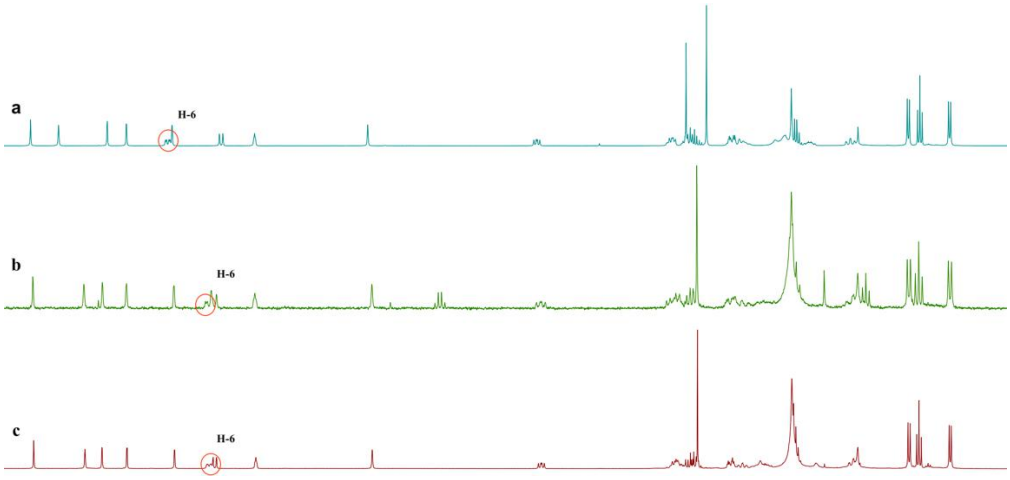

Figure 4. Comparison of ^{1}H NMR spectra (Recorded at 600 MHz in $CDCl_3$). **a**, ^{1}H NMR spectrum of **2**. **b**, ^{1}H NMR spectrum of mixture after reaction. **c**, ^{1}H NMR spectrum of **1**.

Considering the interesting anti-cancer activities displayed by sclerophytin A and pachycladin A [7,9], all isolates were carried out the tests of cytotoxic effects on A549 (Human lung cancer) tumor cells and EGFR inhibitory activities, while none of them showed obvious bioactivities. By comparing the structures of our isolated compounds with those of the most bioactive sclerophytin A and pachycladin A, it seems that the esterification of the hydroxyls, the site of the esterification and the length of the ester would influence the activity. Therefore, the selective hydrolysis of the isolated compounds may result in some sclerophytin A and pachycladin A like anti-cancer drug candidates. However, the scarcity of the isolates prevented the further chemical correlation. We then tried to do an intensive molecular docking analysis to study the SAR, aiming to give an insight for the future structural modification.

On the basis of the speculation on the SAR, sclerophytin A, pachycladin A and litophynol C (**1**) were selected to perform a detailed molecular docking analysis. The highly resolved EGFR crystal structure (PDB codes: 5X2A with a resolution of 1.85Å) was used to investigate the possible binding modes of the three compounds within the catalytic domain of EGFR by means of the Discovery Studio software (Figure 5). Pachycladin A was occupied the same region as 7XO, and its C-6 and C-7 hydroxy participated in hydrogen bonds with Cys797 or Asn842, Lys745 and Asp855 of the EGFR crystal structures 5X2A (Figure 5B, upper row). Stirringly, these four residues were lay in active sites of the kinase. For sclerophytin A, Ser720 and ARG841 were combined by three hydrogen bonds, while C-8 carbonyl of litophynol C (**1**) was the only group

participated in hydrogen bond with Lys745 (Figure 5A and C, upper rows). Furthermore, C-3 acetate and C-11 butyrate of pachycladin A fully occupied the hydrophobic pocket, which promoted Van der Waals inter actions with Leu718, Ser719, Ser720, Gly724, Asp800, Arg841, Asn842, Leu844, Thr854, and Asp855 (Figure 5B, mid and lower row). The lower binding affinity of compound **2**, compared to that of pachycladin A, could be deemed to be related to the position and the length of the ester, which may influence the interaction with hydrophobic pocket and explained why our isolates did not show obvious EGFR inhibitory activity. Although sclerophytin A has been previously reported to be super cytotoxic against mouse lymphocytic leukemia L1210 cells, it displayed less binding affinity than pachycladin A, indicating that it might be less effective on non-small cell lung cancer, and worth for further validation and target fishing.

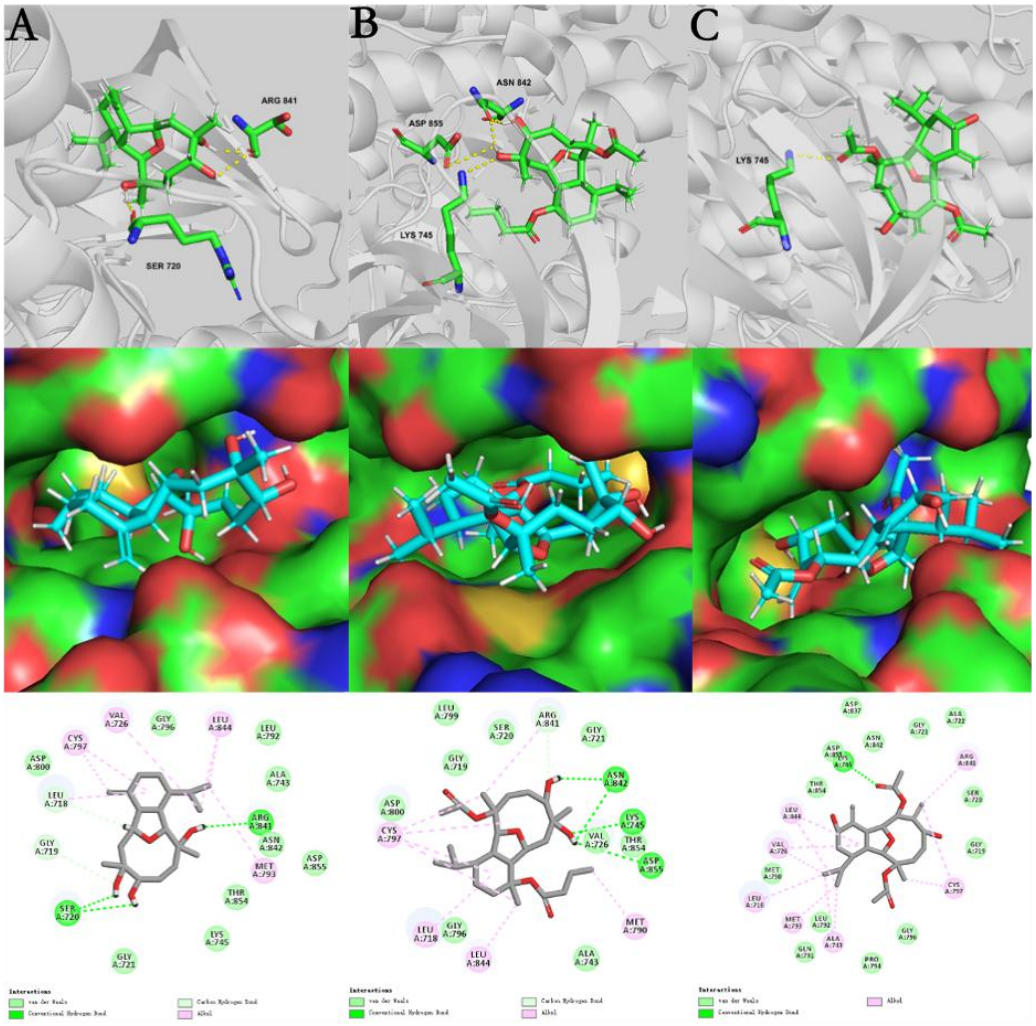

Figure 5. In silico binding mode of sclerophytin A, pachycladin A and litophynol C (**1**) at EGFR kinase crystal structure 5X2A. Upper row: The transparent protein surface, in light gery color, and three compounds shown as sticks with atoms colored C cyan, N blue, O red, and H white, are shown to emphasize the clear combination of hydrogen bonds within the target pocket. Mid row: Surfaces of 5X2A with combined compounds. Lower row: Two-dimensional ligand interaction diagrams of three compounds at the EGFR kinase domain.

3. Discussion

In summary, this is the first time detailed chemical investigation of *C. krempfi* from Ximao island in South China Sea. Two new cladiellin-type diterpenoids, litophynols C and D (**1** and **2**), and four known related compounds **3** – **6** were isolated and fully

elucidated. The stereochemistry of the new compounds was unambiguously determined by extensive spectroscopic analysis, X-ray diffraction analysis, and/or chemical correlation. The discovery of **1** and **2** has expanded the diversity and complexity of marine diterpenes. In bioassay, the results obtained were somewhat disappointing since none of the tested compounds are bioactive, while the SAR of these type of molecules, both isolated and previously reported ones, were studied with the assistance of molecular docking analysis, which has given us a clue for the further structure modification of cladiellin-type diterpenoids towards anti-cancer drug leads.

4. Materials and Methods

4.1. General Experimental Procedures

1D and 2D NMR spectra were recorded on Bruker AVANCE III 500 (125 MHz) and Agilent 1260 Prospekt 2 Bruker Ascend 600 (600 MHz) in $CDCl_3$ using solvent signals as internal standards (CHCl3, δ_H 7.26 ppm; δ_C 77.16 ppm). IR spectra were recorded on a Nicolet 6700 spectrometer (Thermo Scientific, Waltham, MA, USA) with a KBr ATR plate. CD spectra were recorded on a J-815 instrument. Optical rotations were measured on a Perkin-Elmer 241-MC polarimeter (PerkinElmer, Fremont, CA, USA). Melting point was measured on an X-4 digital micromelting point apparatus. LR-ESIMS and HR-ESIMS data were recorded on a Bruker Daltonics Esquire 3000 plus instrument (Bruker Daltonics K. K., Kanagawa, Japan) and a Waters Q-TOF Ultima mass spectrometer (Waters, MA, USA). Commercial silica gel (100-200, 200-300 and 300-400 mesh; Qingdao China) and Sephadex LH-20 gel (Amersham Biosciences) were used for column chromatography (CC). Precoated SiO_2 plates (HSGF-254, Yan Tai Zi Fu Chemical Group Co. Yantai, China) were used for analytical TLC. Semi-preparative HPLC was performed on an Agilent-1260 system equipped with a DAD G1315D detector at 210 and 254 nm using ODS-HG-5 (250mm × 9.4mm, 5μm) by eluting with CH_3CN-H_2O system at 3 mL/min. All solvents used for CC and HPLC were of analytical grades (Shanghai Chemical Reagents Co., Ltd) and chromatographic grade (Dikma Technologies Inc.), respectively.

4.2. Biological Materia

The soft coral specimen, identified as C. krempfin by Prof. Xiu-Bao Li from Hainan University, was collected along the coast of Ximao Island, Hainan Province, China, in 2019, at a depth of -15m. A voucher specimen (NO. 19XD-6) is available for inspection at the Shanghai Institute of Materia Media, Chinese Academy of Sciences.

4.3. Extration and Isolation

The Freeze-dried animals (96g, dry weight) were cut into pieces and exhaustively extracted with acetone at room temperature (5 × 1L). The acetone extract was evaporated to yield a brown residue, which was then partitioned between Et_2O and H_2O. The upper layer was concentrated under reduced pressure to obtain a brown residue 3.6g, which was separated by gradient silica gel column chromatography (200-300 mesh, 0% to 100% Et_2O in petroleum ether), yielding ten fractions (A-J). Fraction D (182.8 mg) was eluted by Sephadex LH-20 with PE/DCM/MeOH (2:1:1) to give five subfractions (D1-D5). Compound **5** (2.1 mg, t_R= 9.1 min) was obtained from the D2 fraction by RP-HPLC (CH_3CN-H_2O, 80:20, 3.0 ml/min). Fraction E (63.0 mg) was isolated by Sephadex LH-20 (PE/DCM/MeOH, 2: 1: 1) to get four subfractions (E1-E4). Each of subfractions E2-E4 were further purified by RP-HPLC under the same elution gradient (CH_3CN-H_2O, 80:20, 3.0 ml/min). The former subfraction E2 yielded compound **4** (2.0 mg, t_R= 21.5 min). Compound **1** (1.4mg, t_R= 6.8 min) was obtained from the midst subfraction E3. The latter subfraction E4 to give compound **2** (5.7mg, t_R= 7.4 min). Fraction F (220.2 mg) was analysed by a column of Sephadex LH-20 eluted with CH_2Cl_2 to get six subfractions (F1-F6). Compound **6** (1.0 mg, t_R= 9.4 min) was yielded from subfraction F3. Compound **3** (2.2 mg, t_R= 9.0 min) was obtained by series of CC from fraction G (363.6 mg).

Litophynol C (**1**). Colorless crystal, mp 183-184 ℃; $[\alpha]_D^{20}$ 24.9 (c 0.14, $CHCl_3$); IR (KBr) υ_{max}/cm^{-1}: 3471, 2924, 2353, 1725, 1254, 1071, 1031; for ^1H NMR ($CDCl_3$, 400 MHz) and ^{13}C NMR ($CDCl_3$, 125MHz) spectral data, see Table 1; HR-ESIMS *m*/*z* 487.2671 $[M + Na]^+$ (calcd. for $C_{26}H_{40}O_7$, 487.2666).

Litophynol D (**2**). Colorless oil; $[\alpha]_D^{20}$ 15.8 (c 0.57, $CHCl_3$); IR (KBr) υ_{max}/cm^{-1}: 3455, 2950, 1724, 1249, 1069, 1034; for ^1H NMR ($CDCl_3$, 400 MHz) and ^{13}C NMR ($CDCl_3$, 125MHz) spectral data, see Table 1; HR-ESIMS *m*/*z* 503.2618 $[M + Na]^+$ (calcd. for $C_{26}H_{40}O_8$, 503.2615).

4. X-ray Crystal Structure Analysis of 1

$C_{26}H_{40}O_7$, M_r = 464.58, monoclinic, crystal size 0.15 × 0.08 × 0.05 mm^3, space group $P2_1$, a = 6.3306(2) Å, b = 43.1346(13) Å, c = 10.1469(3) Å, V = 2643.23(14) $Å^3$, Z = 4, ϱ_{calcd} = 1.167 g/cm^3, F(000) = 1008.0, 22999 collected reflections, 10102 independent reflections (R_{int} = 0.0671, R_{sigma} = 0.0823), final R_1 = 0.1189(wR_2 = 0.3028) reflections with $I \geq 2\sigma$ (I), R_1 = 0.1270, wR_2 = 0.3080 for all unique data. The X-ray measurements were made on a Bruker D8 Venture X-ray diffractometer with Cu Kα radiation (λ = 1.54178 Å) at 170.0 K. The structure was solved with the ShelXT [21] structure solution program using Intrinsic Phasing and refined with the ShelXL [22] refinement package using Least Squares minimisation. Crystallographic data for **1** has been deposited at the Cambridge Crystallographic Data Centre (Deposition nos. CCDC 2074984). Copies of these data can be obtained free of charge via www.cdcc.cam.ac.uk/conts/retrieving.html or from the Cambridge Crystallographic Data Centre, 12 Union Road, Cambridge CB21EZ, UK. [Fax: (+44) 1223-336-033. E-mail: deposit@ccdc.cam.ac.uk.]

5. Bioassay Procedures

5.1. EGFR activity assays

6 compounds were screened on EGFR used staurosporine obtained from MedChemExpress (Cat. No. HY-15141; Lot. No. 41248) as the reference compound. In the bioassay for EGFR, testing kinases were performed in 1x kinase base buffer containing 50 mM HEPES (pH 7.5) and 0.0015% Brij-35, and stop buffer containing 100 mM HEPES (pH 7.5), 0.0015% Brij-35, 0.2% Coating Reagent #3, and 50 mM EDTA. For the compound preparing part, compounds were diluted to 50X of the final desired highest inhibitor concentration in reaction by 100% DMSO, and 100 µl of the compound dilution was transferred to a well in a 96-well plate. Besides, 100 µl of 100% DMSO was added to two empty wells for no compound control and no enzyme control in the same 96-well plate which was marked as source plate. Then, 10 µl of compound from source plate were transferred to a new 96-well plate as the intermediate plate which each well contained 90 µl of 1x kinase buffer. The compounds were mixed in intermediate plate for 10 min on shaker. For assay plate, 5 µl of each well from the 96-well intermediate plate was transferred to a 384-well plate in duplicates. For kinase reaction, 2.5x enzyme solution and 2.5x peptide solution were prepared. And 5 µl of compound were settled in assay plate with 10% DMSO. Besides, 10 µl of 2.5x enzyme solution was added to each well of the 384-well assay plate that was incubated at room temperature for 10 min. Then, 10 µl of 2.5x peptide solution to each well of the 384-well that was incubated at 28 ℃ for 30 min and stopped by 25 µl stop buffer. Percent inhibition was estimated using max-conversion divided by max-min, which inhibition values were converted by convert conversion values from caliper program. IC50 values were obtained from fitting the data in XLfit excel add-in version 4.3.1.

5.2. Anti-tumor assays

Anti-tumor assays were carried out using A549 (Human lung cancer) tumor cells, following a previously described procedure for a modification of the MTT colorimetric method [23,24], with 5-fluorouracil used as the positive control. To measure the

anti-proliferative activity of tested compounds, three concentrations with three replications were performed on cell line.

6. Molecular docking

The cocrystal structure of EGFR (PDB code 5X2A) was obtained from RCSB Protein Data Bank. The water molecules were removed in Discovery Studio (DS), while the binding site of sclerophytin A, pachycladin A and litophynol C (**1**) on the EGFR receptor was consistent with that of 7XO. And the combined spherical area was x = 3.789, y = 17.478, z = -29.936, Radius = 10.85. Using protein preparation tool in DS, the receptor was prepared for docking. Ligands were sketched in ChemBioDraw program and uploaded to DS. Furthermore, optimized ligands were obtained through prepare ligands tool and minimize ligands tool. The molecular docking module (CDOCKER) was used for docking, and the simulation with the highest -CDOCKER INTERACTION ENERGY score was analyzed and visualized in Pymol [25,26].

Supplementary Materials: The following supporting information can be downloaded at: www.mdpi.com/xxx/s1, Figure S1: ^{1}H NMR spectrum of compound **1** (600 MHz, $CDCl_3$); Figure S2: ^{13}C NMR spectrum of compound **1** (125 MHz, $CDCl_3$); Figure S3: DEPT135 spectrum of compound **1** (125 MHz, $CDCl_3$); Figure S4: HSQC spectrum of compound **1** (600 MHz, $CDCl_3$); Figure S5: ^{1}H-^{1}H COSY spectrum of compound **1** (600 MHz, $CDCl_3$); Figure S6: HMBC spectrum of compound **1** (600 MHz, $CDCl_3$); Figure S7: NOESY spectrum of compound **1** (600 MHz, $CDCl_3$); Figure S8: HR-ESI-MS spectrum of compound **1**; Figure S9: IR spectrum of compound **1**; Figure S10: ORD spectrum of compound **1**; Figure S11: ^{1}H NMR spectrum of compound **2** (600 MHz, $CDCl_3$); Figure S12: ^{13}C NMR spectrum of compound **2** (125 MHz, $CDCl_3$); Figure S13: DEPT135 spectrum of compound **2** (125 MHz, $CDCl_3$); Figure S14: HSQC spectrum of compound **2** (600 MHz, $CDCl_3$); Figure S15: ^{1}H-1H COSY spectrum of compound **2** (600 MHz, $CDCl_3$); Figure S16: HMBC spectrum of compound **2** (600 MHz, $CDCl_3$); Figure S17: NOESY spectrum of compound **2** (600 MHz, $CDCl_3$); Figure S18: HR-ESI-MS spectrum of compound **2**; Figure S19: IR spectrum of compound **2**; Figure S20: ORD spectrum of compound **2**; Figure S21: ^{1}H NMR spectrum of compound **3** (400 MHz, $CDCl_3$); Figure S22: ^{13}C NMR spectrum of compound **3** (125 MHz, $CDCl_3$);Figure S23: ^{1}H NMR spectrum of compound **4** (400 MHz, $CDCl_3$); Figure S24: ^{13}C NMR spectrum of compound **4** (125 MHz, $CDCl_3$);Figure S25: ^{1}H NMR spectrum of compound **5** (500 MHz, $CDCl_3$); Figure S26: ^{13}C NMR spectrum of compound **5** (125 MHz, $CDCl_3$);Figure S27: ^{1}H NMR spectrum of compound **6** (500 MHz, $CDCl_3$); Figure S28: ^{13}C NMR spectrum of compound **6** (125 MHz, $CDCl_3$);Figure S29: ^{1}H NMR spectrum of mixture (600 MHz, $CDCl_3$); Figure S30: HR-ESI-MR spectrum of mixture.

Author Contributions: Y.-W.G. and X.-W.L. conceived and designed the experiments; Y.J. performed the experiments and analyzed the data; L.-G.Y. contributed materials; Y.-W.G., X.-W.L., and Y.J. wrote the paper.

Funding: The research work was financially supported by the National Key Research and Development Program of China (No. 2021YFF0502400), the National Natural Science Foundation of China (Nos. 42076099, 81991521, and 82022069), the Shanghai Rising-Star Program (No. 20QA1411100), "Youth Innocation Promotion Association" of Chinese Academy of Sciences (No. Y202065), and the SKLDR/SIMM Project (No. SIMM2103ZZ-06).

Institutional Review Board Statement: Not applicable.

Data Availability Statement: Data are contained within the article or Supplementary Material.

Acknowledgments: We thank Prof. Xiu-Bao Li from Hainan University for the taxonomic identification of the soft coral material.

Conflicts of Interest: The authors declare no conflict of interest.

References

1. Chill, L.; Berrer, N.; Benayahu, Y.; Kashman, Y. Eunicellin Diterpenes from Two Kenyan Soft Corals. *J. Nat. Prod.* **2005**, *68*, 19-25.

2. Li, G.; Dickschat, J. S.; Guo, Y.W. Diving into the world of marine 2,11-cyclized cembranoids: a summary of new compounds and their biological activities. *Nat. Prod. Rep*. **2020**, *37*, 1367-1383.
3. Tai, C.J.; Su, J.H.; Huang, M.S.; Wen, Z.H.; Dai, C.F.; Sheu, J.H. Bioactive Eunicellin-Based Diterpenoids from the Soft Coral *Cladiella krempfi*. *Mar. Drugs.* **2011**, *9*, 2036-2045.
4. Raveendran, T.V.; Mol, V.P. Limna; Parameswaran, P.S. Natural Product Antifoulants from the octocotals of Indian waters. *Int. Biodeter. Biodegr*. **2011**, *65*, 265-268.
5. Cai, Y.S.; Yao, L.G.; Pascale, A.D.; Irace, C.; Mollo, E.; Taglialatela-Scafati, O.; Guo, Y.W. Polyoxygenated diterpenoids of the eunicellin-type from the Chinese soft coral *Cladiella krempfi*. *Tetrahedron.* **2013**, *69*, 2214-2219.
6. Huang, T.Z.; Chen, B.W.; Huang, C.Y.; Hwang, T.L.; Dai, C.F., Sheu, J.H. Eunicellin-Based Diterpenoids, Hirsutalins N-R, from the Formosan Soft Coral *Cladiella hirsuta*. *Mar. Drugs.* **2014**, *12*, 2446-2457.
7. Alam, M.; Sharma, P.; Zektzer, A.S.; Martin, G.E.; Ji, X.; Van der Helm, D.J. Sclerophytin C-F: Isolation and Structures of Four New Diterpenes from the Soft Coral *Sclerophytum capitalis*. *J. Org. Chem.* **1989**, *54*, 1896-1900.
8. Yue, G.Z.; Zhang, Y.; Fang, L.C.; Li, C.C.; Luo, T.P.; Yang, Z. Collective Synthesis of Cladiellins Based on the Gold-Catalyzed Cascade Reaction of 1,7-Diynes. *Angew. Chem. Int. Ed.* **2014**, *53*, 1837-1840.
9. Mohyeldin, M.M.; Akl, M.R.; Siddique, A.B.; Hassan, H.M.; El Sayed, K.A. The marine-derived pachycladin diterpenoids as novel inhibitors of wild-type and mutant EGFR. *Biochem. Pharmacol*. **2017**, *126*, 51-68.
10. Li, G.; Li, H.; Tang, W.; Guo, Y.W.; Li. X.W. Klyflaccilides A and B, Diterpenoids with 6/5/8/3 Fused Tetracyclic Carbon Skeleton from the Hainan Spft Coral *Klyxum flaccidum*. *Org. Lett*. **2019**, *21*, 5660-5664.
11. Yin, F.Z.; Huan, X.J.; Mudianta I.W.; Miao, Z.H.; Wang, H.; Guo, Y.W.; Li, X.W. Polyoxygenated Cembranoids from Soft Coarl *Lobophytum Crassum* and Their Anti-tumoral Activities. *Chin. J. Chem.* **2021**, *39*, 640-646.
12. Xue, D.Q.; Liu, H.L.; Chen, S.H.; Mollo, E.; Gavagnin, M.; Li, J.; Li, X.W.; Guo, Y.W. 5-Alkylpyrrole-2-carboxaldehyde derivatives from the Chinese sponge *Mycale lissochela* and their PTP1B inhibitory activities. *Chinese Chem. Lett*. **2017**, *28*, 1190-1193.
13. Li, Y.F.; Li, S.W.; Cuadrado, C.; Gao, C.L.; Wu, Q.H.; Li, X.L.; Pang, T.; Daranas, A.H.; Guo, Y.W.; Li, X.W. Polyoxygenated anti-inflammatory biscembranoids from the soft coral *Sarcophyton tortuosum* and their stereochemistry. *Chinese Chem. Lett*. **2021**, *32*, 271-276.
14. Chen, B.; Huan, X.J.; Miao, Z.H.; De Voogd, N.J.; Gu, Y.C.; Wang, C.Y.; Guo, Y.W.; Li, X.W. Uncommon Bis-quinolizidine Alkaloids from the Hainan Sponge *Neopetrosia chaliniformis*. *Chin. J. Chem*. **2021**, *39*, 1838-1842
15. Ru, T.; Cai, Y.S.; Li, H.; Tang, W.; Wang, H.; Guo, Y.W. Further new eunicellin-based diterpenoids from the Guangxi Weizhou soft coral *Cladiella krempfi*. *Fitoterapia*, **2018**, *131*, 200-203.
16. Sun, L.L.; Li, W.S.; Li J.; Zhang, H.Y.; Yao, L.G.; Luo, H.; Guo, Y.W.; Li, X.W. Uncommon Diterpenoids from the South China Sea Soft Coral *Sinularia humilis* and Their Stereochemistry. *J. Org. Chem.* **2021**, *86*, 3367-3376.
17. Chen, Z.H.; Li, W.S.; Zhang, Z.Y.; Luo, H.; Wang, J.R.; Zhang, H.Y.; Zeng, Z.R.; Chen, B.; Li, X.W.; Guo, Y.W. Sinusiaetone A, an Anti-inflammatory Norditerpenoid with a Bicyclo[11.3.0]hexadecane Nucleus from the Hainan Soft Coral *Sinularia siaesensis*. *Org. Lett.* **2021**, *23*, 5621-5625.
18. Zeng, Z.R.; Li, W.S.; Nay, B.; Hu P.; Zhang, H.Y.; Wang, H.; Li, X.W.; Guo, W.Y. Sinunanolobatone A, an Anti-inflammatory Diterpenoid with Bicyclo[13.1.0]pentadecane Carbon Scaffold, and Related Casbanes from the Sanya Soft Coral *Sinularia nanolobata*. *Org. Lett*. **2021**, *23*, 7575-7579.
19. Miyamoto, T.; Yamada, K.; Ikeda, N.; Komori, T.; Higuchi, R. Bioactive terpenoids from Octocorallia, I. Bioactive diterpenoids: Iitophynols A and B from the mucus of the soft coral *Litophyton* sp. *J. Nat. Prod.* **1994**, *57*, 1212-1219.
20. Clark, J.S.; Delion, L.; Farrugia, L. Synthesis of Four Diastereomers of Sclerophytin F and Structural Reassignment of Several Sclerophytin Natural Products. *Chem. Eur. J.* **2015**, *21*, 4772-4780.
21. Sheldrick, G.M. *SHELXT*-Integrated space-group and crystal-structure determination *Acta Cryst*. **2015**, *A71*, 3-8.
22. Sheldrick, G.M. Crystal structure refinement with *SHELXL*. *Acta Cryst*. **2015**, *C71*, 3-8.
23. Hansen, M.B.; Nielsen, S.E.; Berg, K. Re-examination and Futuer Development of a Precise and Rapid Dye Method for Measuring Cell Growth/cell Kill. *J. Immunol. Methods*. **1989**, *199*, 203-210.
24. Mosmann, T. Rapid Colorimetric Assay for Cellular Growth and Survival: Application to Proliferation and Cytotoxicity Assays. *J. Immunol. Methods*. **1983**, *65*, 55-63.
25. Elkamhawy, A.; Park, J.; Hassan, A.H.E.; Ra, H.; Pae, A.N.; Lee, J.; Park, B.G.; Moon, B.; Park, H.M.; Roh, E.J. Discovery of 1-(3-(benzyloxy) pyridine-2-yl)-3-(2-(piperazin-1-yl) ethyl) urea: A new modulator for amyloid beta-induced mitochondrial dysfunction. *Eur. J. Med. Chem*. **2017**, *128*, 56-69.
26. Wang, S.B.; Liu, H.; Wang, X.K.; Lei, K.; Li, G.Y.; Li, J.; Liu, R.M.; Quan, Z.S. Synthesis of 1,3,4-oxadiazole derivatives with anticonvulsant activity and their binding to the $GABA_A$ receptor. *Eur. J. Med. Chem*. **2020**, *206*, 112672.